2007

# Development of Ruthenium-Based Catalysts for Oxygen Reduction Reaction

Lingyun Liu
*University of South Carolina - Columbia*

Hansung Kim
*Yonsei University, Seoul, South Korea*

Jong-Won Lee
*University of South Carolina - Columbia*

Branko N. Popov
*University of South Carolina - Columbia*, popov@engr.sc.edu



## Publication Info

*Journal of the Electrochemical Society*, 2007, pages A123-A128.

*Journal of The Electrochemical Society*, **154** (2) A123-A128 (2007)
0013-4651/2006/154(2)/A123/6/$20.00 © The Electrochemical Society



# Development of Ruthenium-Based Catalysts for Oxygen Reduction Reaction

**Lingyun Liu,[a] Hansung Kim,[b,*] Jong-Won Lee,[a] and Branko N. Popov[a,*,z]**

[a]*Center for Electrochemical Engineering, Department of Chemical Engineering, University of South Carolina, Columbia, South Carolina 29208, USA*
[b]*Department of Chemical Engineering, Yonsei University, Seoul, South Korea*

A process was developed to synthesize ruthenium-based chelate ($RuN_x$) electrocatalysts for the oxygen reduction reaction, using $RuCl_3$ and propylene diammine as the Ru and N precursors, respectively. High-temperature pyrolysis has a critical role in the formation of the catalytic Ru–N sites for oxygen reduction. The $RuN_x$ catalyst modified in the presence of nitrogen-containing organic exhibited comparable catalytic activity and selectivity for oxygen reduction to the carbon-supported Pt catalyst in acidic media. The catalyst generates less than 2% hydrogen peroxide during oxygen reduction.
 [DOI: 10.1149/1.2402108] 

Manuscript submitted May 4, 2006; revised manuscript received September 12, 2006. Available electronically December 26, 2006.

A major impediment to the commercialization of fuel cells is the low activity of electrocatalysts for oxygen reduction which involves multiple electron transfer steps. Platinum is considered the best cathode catalyst toward four-electron reduction of oxygen to water in acidic environments.[1-4] It also shows the lowest overpotential and the highest stability. However, Pt remains an expensive metal of low abundance, and it is thus of great interest to find Pt-free metal alternatives used for proton exchange membrane (PEM) fuel cells.

Recently, there has been considerable research on Ru-based chalcogenides[5,6] and macrocyclic compounds of transition metal.[7] Alonso-Vante et al.[5] were the first to demonstrate that Ru-based chalcogenides of chevrel-phase type (e.g., $Mo_4Ru_2Se_8$) show significant catalytic activity for oxygen reduction in acidic media and catalyze the four-electron reduction reaction of $O_2$ to $H_2O$. However, the chevrel-phase chalcogenides are typically synthesized by a solid-state reaction of pure elements at high temperatures of 1200–1700°C, which makes the synthesis procedure very complicated and costly. In order to circumvent those problems, low-temperature methodologies have been developed to prepare amorphous chalcogenides (e.g., $Mo_xRu_ySe_z$ and $Ru_xSe_y$) by using metal carbonyls;[8] the solubility of Se is as low as 22.8 μM,[9] which restricts the mass production of the compounds and also results in a long synthesis period.

Since Jasinski's discovery of the catalytic properties of Co phthalocyanines,[10] various kinds of macrocyclic compounds have been synthesized using nonprecious transition metals such as Fe, Co, Ni, Cu, Zn, V, and Mn.[11] The central metal ion in the macrocycle may play a crucial role in the oxygen reduction reaction. Some Fe-macrocyclic compounds supported on carbon showed comparable activity to Pt/C; however, they exhibit low electrochemical stability in acidic environments.[12] It has been reported that the Co-macrocyclic compounds exhibit higher electrochemical stability compared with the Fe complexes, but they catalyze two-electron reduction of $O_2$ to $H_2O_2$.[13]

In this work, a methodology was developed to synthesize carbon-supported Ru-chelate catalyst. The synthesized catalysts were subjected to extensive materials characterization studies such as X-ray photoelectron spectroscopy (XPS), X-ray diffractometry (XRD), and transmission electron microscopy (TEM). Rotating ring disk electrode (RRDE) technique was performed to evaluate the selectivity to four-electron reduction as well as the catalytic activity toward oxygen reduction. The performances of Ru-based catalysts prepared using various synthesis methodologies were also evaluated and compared in terms of the catalytic activity and selectivity.

* Electrochemical Society Active Member.
z E-mail: popov@engr.sc.edu

## Experimental

*Preparation of $RuN_x$ catalysts*.— The desired amount of $RuCl_3$ was dissolved in isopropyl alcohol (100 mL). The solution was refluxed at 80–90°C under stirring conditions. Next, propylene diammine was added into the solution to form Ru–N complexes, followed by the addition of carbon black powders (0.4 g, Ketjen Black). The mixture was refluxed for several hours and then dried under vacuum at 80°C. The resulting powder specimens were heat-treated in an argon atmosphere at various temperatures ranging from 600 to 900°C.

*Materials characterizations*.— XPS was conducted with a Kratos AXIS 165 high-performance electron spectrometer using a monochromatic Al Kα radiation. Low-resolution survey scans were conducted with a step size of 0.5 eV and a dwell time of 100 ms. Next, high-resolution scans were acquired in N 1 s region using a 0.1 eV step size and a 300 ms dwell time. In order to identify the crystal structures of the synthesized catalysts, XRD patterns were recorded with an automated Rigaku diffractometer using Cu Kα radiation over the scanning angle range of 10–60° at the scan rate of 4° $min^{-1}$. To determine the particle size of the catalyst, TEM was performed using a Hitachi H-8000 operated at 200 keV.

*Electrochemical characterizations*.— The RRDE measurements were performed in a three-electrode electrochemical cell using a bipotentiostat (Pine Instruments) at room temperature. An RRDE with gold ring (5.52 mm inner diam and 7.16 mm outer diam) and glassy carbon disk (5.0 mm diam) was employed as the working electrode. The catalyst ink was prepared by blending the catalyst powder (8 mg) with isopropyl alcohol (1 mL) in an ultrasonic bath. The catalyst ink (15 μL) was deposited onto the glassy carbon disk, which was previously polished with $Al_2O_3$ powder. After drying, 10 μL of a mixture of Nafion solution (5 wt %, Aldrich) and isopropyl alcohol was coated onto the catalyst layer to ensure better adhesion of the catalyst on the glassy carbon substrate. The electrolyte was 0.5 M $H_2SO_4$ solution. A platinum mesh and an $Hg/HgSO_4$ electrode were used as the counter and reference electrodes, respectively. All potentials in this work were referred to a normal hydrogen electrode (NHE).

In order to estimate the double-layer capacitance, the electrolyte was deaerated by bubbling with $N_2$, and the cyclic voltammogram was recorded by scanning the disk potential between 0.04 and 1.04 V (NHE) at rate of 5 mV $s^{-1}$. Then, the electrocatalytic activity for oxygen reduction was evaluated in the oxygen-saturated electrolyte. The oxygen reduction current was taken as the difference between currents measured in the deaerated and oxygen-saturated electrolytes. The ring potential was held at 1.2 V (NHE) to oxidize $H_2O_2$ generated during the oxygen reduction reaction.

The Koutecky-Levich equation[14] was used to calculate the kinetically limited current $I_k$

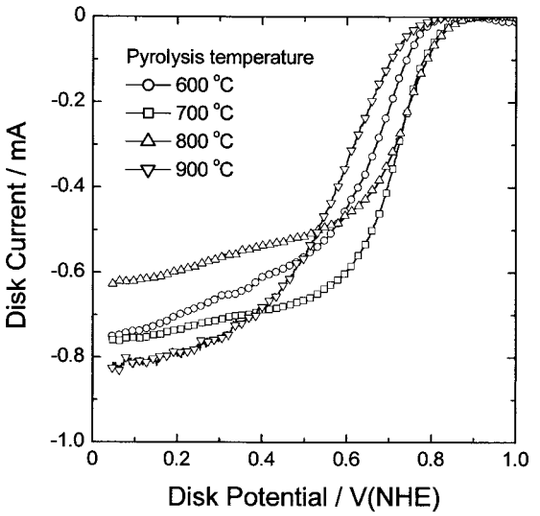


**Figure 1.** Polarization curves on the rotating disk electrodes for the $RuN_x$/C catalysts pyrolized at 600–900°C. The measurements were performed in 0.5 M $H_2SO_4$ solution saturated with oxygen at the potential scan rate of 5 mV $s^{-1}$ and the rotation speed of 900 rpm.

$$\frac{1}{I_d} = \frac{1}{I_k} + \frac{1}{I_l} + \frac{1}{I_f} = \frac{1}{nFAkC_{O_2}} + \frac{1}{0.2\,nFAD_{O_2}^{2/3}\omega^{1/2}v^{-1/6}C_{O_2}} + \frac{L}{nFAC_fD_f} \quad [1]$$

where $I_d$ is the measured disk current, $I_l$ the diffusion limited current, $I_f$ the Nafion film diffusion limited current, $n$ the number of electrons exchanged in the electrochemical reaction, $F$ the Faraday constant, $A$ the geometric surface area, $C_{O_2}$ the bulk concentration of oxygen, $D_{O_2}$ the diffusion coefficient of oxygen in the bulk solution, $\omega$ the rotation rate in rpm, $v$ the kinematic viscosity of the solution, $L$ the Nafion film thickness, $C_f$ the reactant concentration in the Nafion film, and $D_f$ means the diffusion coefficient of oxygen in the Nafion film. Because the film thickness was reduced to the extent that $I_f$ becomes significantly larger than $I_k$ and $I_l$, the influence of $I_f$ on the measured current in our experiments was negligible. By plotting $I_d^{-1}$ vs $\omega^{-1/2}$ and extending the regression line, the $y$-intercept or the inverse of $I_k$ can be calculated.

## Results and discussion

*Formation of active reaction sites on $RuN_x$/C catalysts.*— Figure 1 shows polarization curves on the rotating disk electrodes for the carbon-supported $RuN_x$ catalysts pyrolized at various temperatures. The temperatures were varied between 600 and 900°C. The measurements were performed in 0.5 M $H_2SO_4$ solution saturated with oxygen by using a potential scan rate of 5 mV $s^{-1}$ and rotation speed of 900 rpm. In this work, the as-refluxed catalyst was found to hardly catalyze oxygen reduction, indicating no formation of the active reaction sites. The RRDE data in Fig. 1 show that the as-pyrolized catalysts exhibit the onset potentials for oxygen reduction as high as 0.85 V (NHE) and the well-defined limiting currents below 0.6 V (NHE). The pyrolysis at 700°C leads to the best performance of the catalyst in terms of the activation overpotential and the reaction kinetics for oxygen reduction.

Table I summarizes the compositions of the as-refluxed and as-pyrolized $RuN_x$/C catalysts determined by XPS. For the as-refluxed catalyst, the Ru concentration evaluated by XPS is much lower than the concentration (20 wt %) in the precursor solution. Keeping in mind that the escape depth of photoelectrons is only a few nanometers, the result suggests that the Ru clusters formed on the carbon support during refluxing may be mostly covered with a graphitic layer. The XPS data also indicate that the high-temperature pyrolysis induces a significant loss of Ru and N, while the O concentration remains almost constant.

**Table I. Surface compositions of the as-refluxed and as-pyrolized $RuN_x$/C catalysts determined by XPS.**

| Element | Concentration (wt %) As-refluxed (before heat treatment) | As-pyrolized (after heat treatment) |
|---|---|---|
| Ru | 4.4 | 1.8 |
| C | 70.3 | 89.9 |
| N | 18.1 | 1.8 |
| O | 7.2 | 7.5 |

Figure 2a and b present the XPS spectra of N 1 s region for the as-refluxed and as-pyrolized $RuN_x$/C catalysts, respectively. The XPS spectrum of the as-refluxed catalyst exhibits a broad peak around 399.8 eV which corresponds to the nitrogen of the ternary amine-type.[15] Upon pyrolysis the peak splits into two broad peaks at about 398.4 and 400.4 eV which can be assigned to two different types of nitrogen on the carbon matrix, namely, the "pyridinic N"

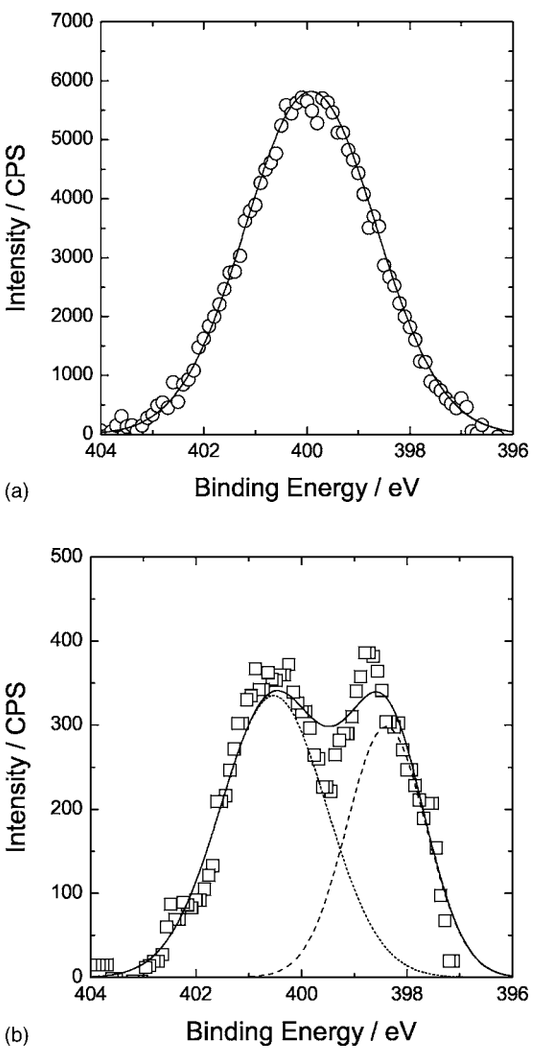


**Figure 2.** XPS spectra of N 1s region for the $RuN_x$/C catalysts (a) as refluxed and (b) as pyrolized.

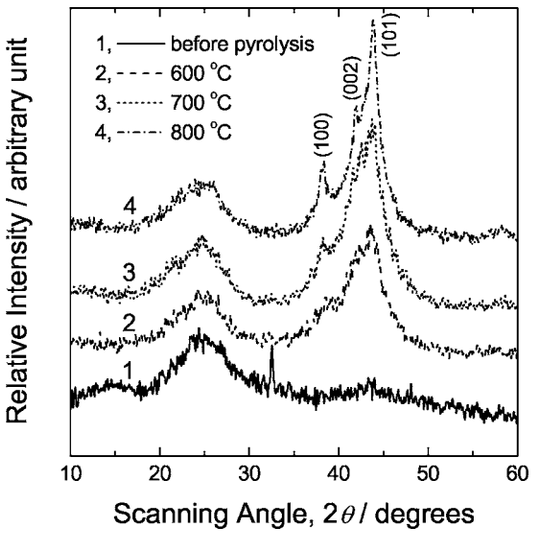


**Figure 3.** XRD patterns of the $RuN_x$/C catalysts subjected to pyrolysis at 600–800°C. For comparison, the XRD pattern for the as-refluxed catalyst is given in the figure.

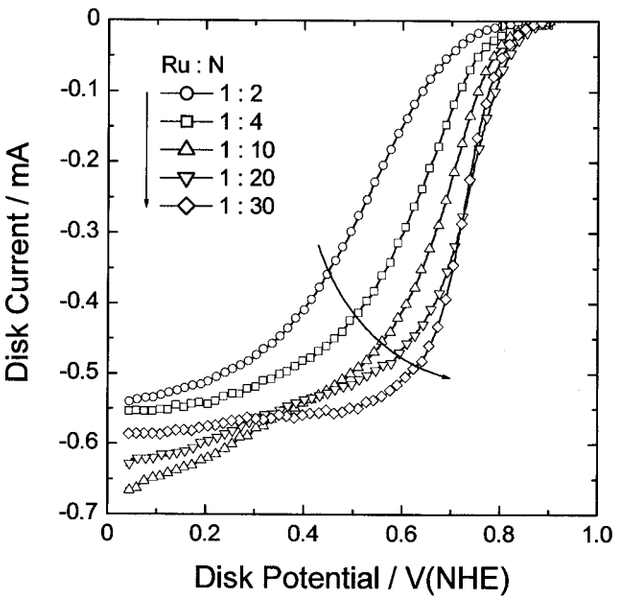


**Figure 4.** Polarization curves on the rotating disk electrodes for the $RuN_x$/C catalysts prepared using different molar ratios of Ru to N in the precursor solution.

and the "pyrrolic N," respectively. It is known that the pyridinic N possesses one lone pair of electrons in addition to the one electron donated to the conjugated $\pi$ bond system, so it provides an orbital in the plane of the graphene layer that is capable for coordinating the metal ions.[16] From the results of RRDE and XPS measurements, it is clear that the high-temperature pyrolysis leads to the formation of Ru clusters coordinated with pyridinic N, and such Ru–N chelate sites are catalytically active for oxygen reduction.

Figure 3 presents the powder XRD patterns of the carbon-supported $RuN_x$ catalysts which were subjected to pyrolysis at various temperatures. For comparison, the XRD pattern for the as-refluxed catalyst is also shown in Fig. 3, and only a broad diffraction peak resulting from carbon support is observed around 24.5°. The absence of the diffraction peaks from Ru indicates that Ru crystal particles are too small to be detected by the instrument. However, all of the XRD patterns for the as-pyrolized catalysts clearly exhibit the characteristic peaks which correspond to crystalline Ru. As indicated in Fig. 3, the diffraction peaks at 38.2, 42.0, and 43.8° are assigned to (100), (002), and (101) planes, respectively.

As the pyrolysis temperature increases from 600 to 800°C, the diffraction peaks of Ru become sharper. That is, the Ru crystallite size gradually increases with increasing pyrolysis temperature, which suggests that lower activity of the as-pyrolized catalyst at 800°C results from the agglomeration of Ru crystallite particles. The results also indicated that the pyrolysis temperature plays a critical role in the formation of the active reaction sites. However, higher temperatures than 700 °C cause Ru crystallite particles to agglomerate, resulting in a loss of the catalytic activity.

*Effect of nitrogen content on the catalytic activity and selectivity of $RuN_x$/C.*— Figure 4 shows typical polarization curves on the rotating disk electrodes for the carbon-supported $RuN_x$ catalysts prepared using different molar ratios of Ru to N in the precursor solution. It is clearly seen that the nitrogen incorporation enhances the catalytic activity toward the oxygen reduction reaction. This fact further confirms that the N-coordinated Ru clusters are catalytically active for oxygen reduction. The catalyst prepared with the Ru/N ratio of 1:20 shows the lowest activation overpotential for oxygen reduction, while the best reduction kinetics is observed on the catalyst with the 1:30 ratio.

The Koutecky-Levich plots obtained at the potential range between 0.5 and 0.7 V (NHE) are presented in Fig. 5 for the catalyst with the Ru/N ratio of 1:20. A linear relationship between $I_d^{-1}$ and $\omega^{-1/2}$ is clearly observed and the slope remains nearly constant, regardless of the potential, which indicates that the electrochemical reaction follows a first-order kinetics.[17] The values of $I_k$ at 0.7 V (NHE) for different Ru/N ratios are listed in Table II. The $I_k$ value increases with increasing the nitrogen content, which confirms that nitrogen incorporation improves the catalytic activity of $RuN_x$/C.

In general, the oxygen reduction reaction proceeds by two pathways as follows[8]

$$\begin{array}{ccccc} & & \overset{1}{\overbrace{\qquad\qquad\qquad}} & & \\ & & \uparrow \qquad\qquad \downarrow & & \\ O_{2,b} & \rightarrow & O_{2,a} \xrightarrow{2} H_2O_{2,a} & \xrightarrow{3} & H_2O \\ & & \downarrow 4 & & \\ & & H_2O_{2,b} & & \end{array} \qquad [2]$$

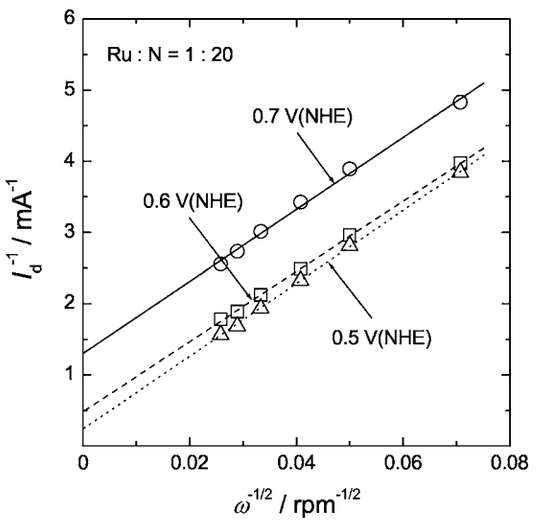


**Figure 5.** Koutecky–Levich plots at different potentials measured on the $RuN_x$/C catalysts prepared with the Ru/N ratio of 1:20.

**Table II. Kinetically limited currents, $I_k$, at 0.7 V (NHE) determined for the $RuN_x$/C catalysts prepared using different molar ratios of Ru to N in the precursor solution.**

| Ru/N | $I_k$ at 0.7 V (NHE) (mA) |
|---|---|
| 1:2 | 0.051 |
| 1:4 | 0.165 |
| 1:10 | 0.331 |
| 1:20 | 0.751 |
| 1:30 | 0.864 |

where subscripts *a* and *b* denote the species adsorbed on the electrode surface and that in the bulk, respectively. $O_2$ may be directly reduced to $H_2O$ through four-electron transfer (Reaction 1). In parallel, $O_2$ may be reduced to $H_2O_2$ via two-electron transfer (Reaction 2), followed by either reduction of $H_2O_2$ to $H_2O$ (Reaction 3) or transport of the adsorbed $H_2O_2$ to the bulk solution (Reaction 4). In the case of metal-chelate catalysts, $H_2O_2$ is believed to be responsible for the deterioration of electrode performance over time, because it may destroy the active reaction sites by oxidation of nitrogen ligands.[18] In addition, the polymer electrolyte membrane may degrade over time due to attack by peroxide radicals.[19]

Figure 6a presents the ring currents measured for the carbon-supported $RuN_x$ catalysts with different molar Ru/N ratios as a function of the disk potential. The ring current increases with decreasing disk potential, then reaches a maximum value between 0.6 and 0.4 V (NHE), and finally decreases with further decreasing the disk potential. The value of ring current decreases with increasing the N content over the whole potential range, which indicates that the nitrogen incorporation improves the selectivity of the catalyst to four-electron reduction of $O_2$ to $H_2O$.

The percentage of $H_2O_2$ produced was calculated using Eq. 3[14] and was plotted in Fig. 6b as a function of the disk potential

$$\%H_2O_2 = \frac{200(I_r/N)}{I_d + (I_r/N)} \quad [3]$$

where $I_r$ and $N$ mean the ring current and the collection efficiency, respectively. Here, the value of $N$ was taken as 0.39. The percentage of $H_2O_2$ generated on the cathode decreases with increasing N content. The $RuN_x$/C catalysts with the Ru-to-N ratios of 1:20 and 1:30 generate less than 2% $H_2O_2$ over the whole potential range, which is much lower than that value reported in the literature.[20]

*Surface-modification of $RuN_x$/C catalysts*.— Organic additive, which contains N and O, was incorporated into the precursor solution during refluxing, in an attempt to increase the catalytic activity and selectivity. Figure 7a and b demonstrates polarization curves on the rotating disk electrodes and the percentage of $H_2O_2$, respectively, measured for the $RuN_x$/C catalyst prepared using urea $[(NH_2)_2CO]$.

It is found that urea has a positive effect on the activation overpotential and the reduction kinetics. The urea-modified $RuN_x$/C catalyst exhibits an onset potential as high as 0.9 V (NHE). Urea chemically modifies the $RuN_x$ catalyst surfaces by providing functional groups of nitrogen and oxygen which contribute to the formation of active reaction sites. Also as presented in Fig. 7b, urea decreases the amount of $H_2O_2$ generated on the cathode.

*Comparative study of Ru-based catalysts synthesized using different methodologies*.— Different types of Ru-based catalysts were synthesized and compared with the $RuN_x$/C catalyst: (*i*) $RuO_x$/C, (*ii*) amorphous $Mo_xRu_ySe_z$/C, and (*iii*) Ru–$NH_3$/C. The $RuO_x$/C catalyst was synthesized by a colloidal method developed in our laboratory.[21] The Ru complex colloidal solution was prepared with a slow addition of $NaHCO_3$ into an aqueous $RuCl_3 \cdot xH_2O$ solution, and then the colloidal particles were adsorbed onto the carbon black under stirring conditions.

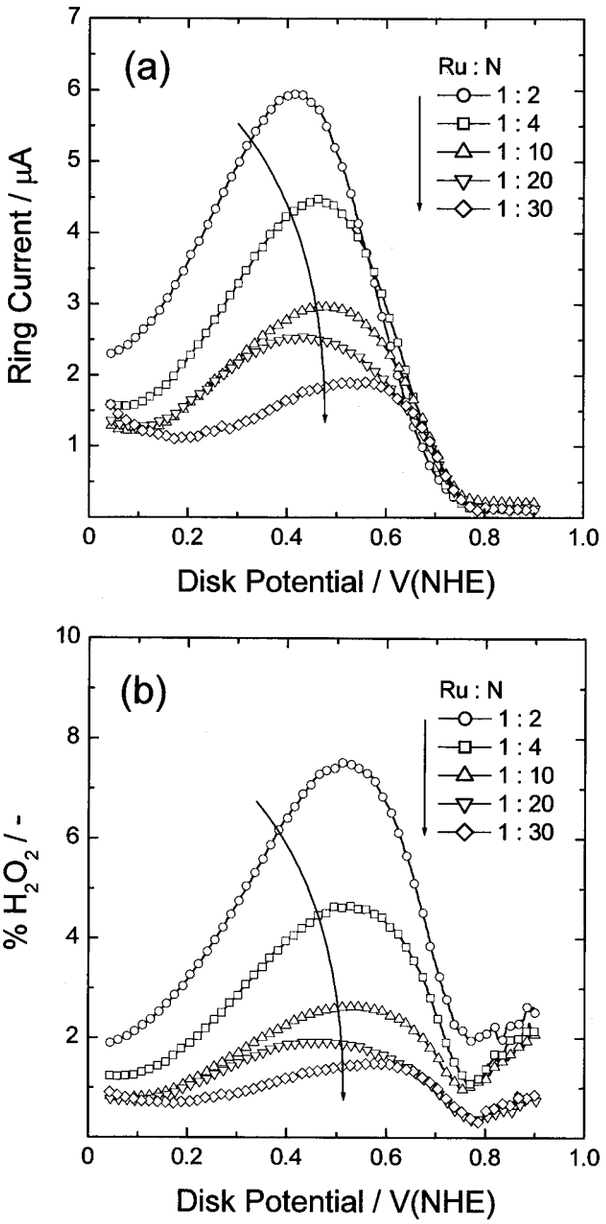


**Figure 6.** (a) Ring currents and (b) $H_2O_2$ percentages determined as a function of the disk potential for the $RuN_x$/C catalysts with different molar Ru/N ratios.

The amorphous $Mo_xRu_ySe_z$/C catalyst was synthesized by reacting metal carbonyls with Se in xylene at 140°C under stirring and refluxing conditions for 20 h, as described by Solorza-Feria and coworkers.[22] Finally, the Ru–$NH_3$/C catalyst was synthesized by heat-treating $Ru^{3+}$-impregnated carbon under an $NH_3$ atmosphere at 800°C for 1 h. Here an $NH_3$ gas was used as the N-precursor instead of propylene diammine.

Figure 8a and b summarizes the polarization curves obtained on the rotating disk electrodes and the percentage of $H_2O_2$, respectively, measured for various Ru-based catalysts. The RRDE data obtained from the commercially available 20 wt % Pt/C catalyst are also given in Fig. 8 for comparison. The urea-modified $RuN_x$/C catalyst shows higher catalytic activity toward the oxygen reduction reaction. As shown in Fig. 8a, the activation overvoltage decreases more than 150 mV when compared with all other Ru-based catalysts

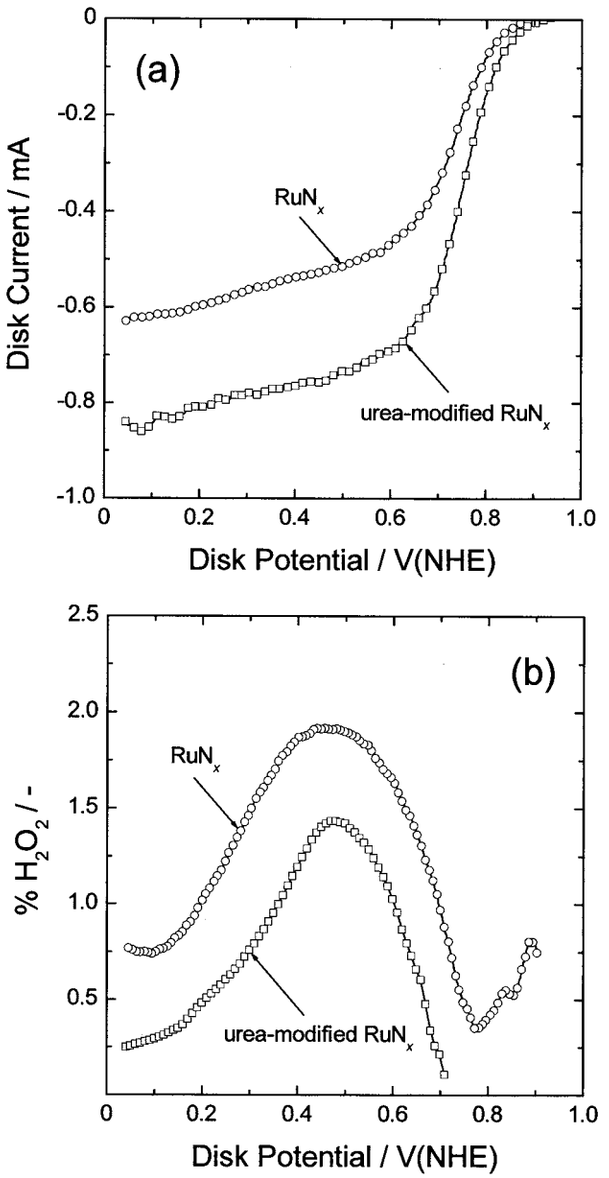


**Figure 7.** (a) Polarization curves on the rotating disk electrodes and (b) $H_2O_2$ percentages measured for the $RuN_x$/C catalysts prepared using urea as an additive.

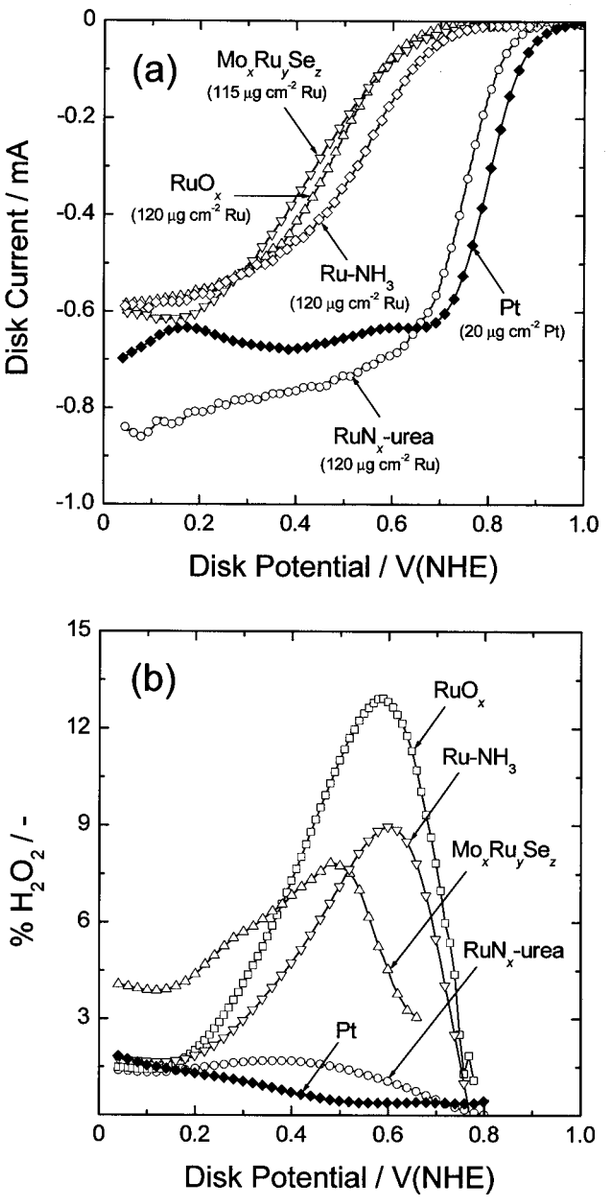


**Figure 8.** (a) Polarization curves on the rotating disk electrodes and (b) $H_2O_2$ percentages measured for various Ru-based catalysts: urea-modified $RuN_x$/C, $RuO_x$/C, amorphous $Mo_xRu_ySe_z$/C and Ru–$NH_3$/C. The RRDE data obtained from the commercial Pt/C is also presented in the figure.

under study. It produces a smaller amount of $H_2O_2$ during oxygen reduction, indicating the enhanced catalytic selectivity toward four-electron reduction. The results indicated that $RuN_x$/C catalyst modified with urea in this work exhibits comparable catalytic activity and selectivity to the commercial Pt/C catalyst in the RRDE tests. From the TEM analysis, the particle sizes of the $RuN_x$ catalysts were estimated to be ca. 2–4 nm, regardless of the presence and absence of urea, which are about two times smaller than the particle sizes of $Mo_xRu_ySe_z$/C and Ru–$NH_3$/C (ca. 4–8 nm).

## Conclusions

Nanosized Ru–N chelate catalysts were synthesized using $RuCl_3$ and propylene diammine, followed by heat treatment at 600–900°C. The influence of pyrolysis temperature, nitrogen content, and surface modifier on the catalytic properties has been investigated. XPS and XRD studies showed that the high-temperature pyrolysis plays a critical role in the formation of the active Ru–N sites, but it causes the agglomeration of Ru crystalline particles above 800°C. The RRDE experiments indicated that the nitrogen incorporation improves the catalytic activity and selectivity toward four-electron reduction of molecular oxygen to water. The urea-modified $RuN_x$/C catalyst with the particle sizes of 2–4 nm exhibited comparable catalytic activity to the carbon-supported Pt catalyst and generated less than 2% $H_2O_2$ during oxygen reduction.

## Acknowledgment

Financial support provided by the Department of Energy (DOE) is gratefully acknowledged.

*University of South Carolina assisted in meeting the publication costs of this article.*

## References


1. M. L. Rao, B. A. Damjanovic, and J. O'M Bockris, *J. Chem. Phys.*, **67**, 2508 (1963).
2. R. R. Adzic, in *Electrocatalysis*, J. Lipkowski and P. Ross, Editor, pp. 197–242, VCH Publishers, New York (1998).
3. N. M. Markovic and P. N. Ross, *Electrochim. Acta*, **45**, 4101 (2000).
4. N. M. Markovic and P. N. Ross, *Surf. Sci. Rep.*, **286**, 1 (2002).
5. N. Alonso-Vante and H. Tributsch, *Nature (London)*, **323**, 431 (1986).
6. R. W. Reeve, P. A. Christensen, A. Hamnett, S. A. Haydock, and S. C. Roy, *J. Electrochem. Soc.*, **145**, 3463 (1996).
7. L. Zhang, J. Zhang, D. P. Wilkinson, and H. Wang, *J. Power Sources*, **156**, 171 (2006).
8. J. Maruyama, M. Inaba, and Z. Ogumi, *J. Electroanal. Chem.*, **458**, 175 (1998).
9. N. Alonso-Vante, H. Tributsch, and O. Solorza-Feria, *Electrochim. Acta*, **40**, 567 (1995).
10. R. Jasinski, *Nature (London)*, **201**, 1212 (1964).
11. K. Wiesener, D. Ohms, V. Neumann, and R. Franke, *Mater. Chem. Phys.*, **22**, 457 (1989).
12. C. Kretzschmar and K. Wiesener, *Elektrokhimiya*, **14**, 1330 (1978).
13. R. Jiang, L. Xu, R. Jin, and S. Dong, *Fenxi Huaxue*, **13**, 270 (1985).
14. U. A. Paulus, T. J. Schmidt, H. A. Gasteiger, and R. J. Behm, *J. Electroanal. Chem.*, **495**, 134 (2001).
15. L. J. Gerenser, J. M. Grace, G. Apai, and P. M. Thompson, *Surf. Interface Anal.*, **29**, 12 (2000).
16. Y. F. Jia, B. Xiao, and K. M. Thomas, *Langmuir*, **18**, 470 (2002).
17. O. Solorza-Feria, S. Ramírez-Raya, R. Rivera-Noriega, E. Ordoñez-Regil, and S. M. Fernández-Valverde, *Thin Solid Films*, **311**, 164 (1997).
18. S. Gupta, D. Tryk, S. K. Zecevic, W. Aldred, D. Guo, and R. F. Savinell, *J. Appl. Electrochem.*, **28**, 673 (1998).
19. S. Lj. Gojković, S. Gupta, and R. F. Savinell, *Electrochim. Acta*, **45**, 889 (1999).
20. H. Schulenburg, M. Hilgendorff, I. Dorbandt, J. Radnik, P. Bogdanoff, S. Fiechter, M. Bron, and H. Tributsch, *J. Power Sources*, **155**, 47 (2006).
21. H. Kim and B. N. Popov, *J. Power Sources*, **104**, 52 (2002).
22. O. Solorza-Feria, K. Ellmer, M. Giersig, and N. Alonso-Vante, *Electrochim. Acta*, **39**, 1647 (1994).